Decay Chain Fitting with a Kalman Filter

Wouter D. Hulsbergen

University of Maryland
Mailing address: Stanford Linear Accelerator Center, P.O. Box 20450, Stanford, CA 94309.

Abstract

We present a method to perform a least squares fit of a decay chain involving multiple decay vertices. Our technique allows for the simultaneous extraction of decay time, position and momentum parameters and their uncertainties and correlations for all particles in a decay chain.

1 Introduction

In high energy physics experiments decay reactions that proceed via intermediate metastable states are usually reconstructed by following a bottom-up approach. One starts by extracting the parameters of those decay vertices from which the reconstructed final state particles emerge and uses the intermediate 'composite' particles for the reconstruction of upstream decays. At each decay vertex the parameters of the composite particle are determined with a least squares fit to its daughter particles, subject to the constraint that those originate from a common point. The disadvantage of this approach, which is sometimes called 'leaf-by-leaf' fitting, is that constraints that are upstream of a decay vertex do not contribute to the knowledge of the parameters of the vertex. An example of a decay for which this is impractical is $K^0_S \to \pi^0\pi^0$.

In this paper we discuss the implementation of a least squares fit that extracts all parameters in a decay chain simultaneously. We shall call this fit, which

Email address: hulsberg@slac.stanford.edu (Wouter D. Hulsbergen).

we developed for data analysis in the *BABAR* experiment, a global decay chain fit. First, we propose a parameterization of a decay chain in terms of vertex positions, momenta and decay times. Subsequently, we argue that the Kalman filter is a suitable technique to extract these parameters and the corresponding covariance matrix from the external constraints, which in the case of *BABAR* are reconstructed charged particle trajectories and neutral particle calorimeter clusters. Finally, we present two examples and briefly summarize experience with the fit in *BABAR*.

The decay chain fits discussed here are hypothesis driven. The task of finding the reconstructed tracks and clusters and associating those with the final state particles in the decay tree is outside the scope of this paper. In *BABAR* physics analyses decay trees are built layer-by-layer, usually by making all possible combinations of final state particles and applying selections on the invariant mass and vertex χ^2. Vertex pattern recognition plays an insignificant role because the low combinatorics does not warrant more complicated algorithms and because the track parameter resolution is barely sufficient to separate the decay vertices of the particles that are of most interest to the experiment, namely B and D mesons.

2 Parameterization of a decay tree

Figure 1 shows a schematic picture of a decay tree. The positions of the vertices in the decay tree, and the momenta of all particles, constitute the degrees of freedom of the decay tree. These degrees of freedom, the internal constraints (such as momentum conservation at each vertex) and the relation to the external reconstruction objects, define the decay tree model.

The choice of parameters in the decay tree model is not unique, but we found the following parameterization suitable for use in *BABAR*. Each reconstructed or 'final state' particle is represented by a momentum vector (p_x, p_y, p_z). The mass of a final state particle is not a parameter in the fit, but assigned based on the particle hypothesis in the decay tree. Each intermediate particle in the decay tree is modeled by a four momentum vector (p_x, p_y, p_z, E) and a decay vertex position (x, y, z). If the composite particle is not at the head of the decay tree, we also assign a parameter for its decay time. We choose this parameter to be $\theta \equiv l/|\vec{p}|$, where l is the decay length.

If a composite particle has an expected decay length much smaller than the vertex detector resolution, we call this particle a 'resonance'. A resonance does not have a decay time parameter and it shares the decay vertex position with its mother, unless it is at the head of the decay tree. In the *BABAR* reconstruction software particles with an expected decay length $c\tau < 1\,\mu$m,

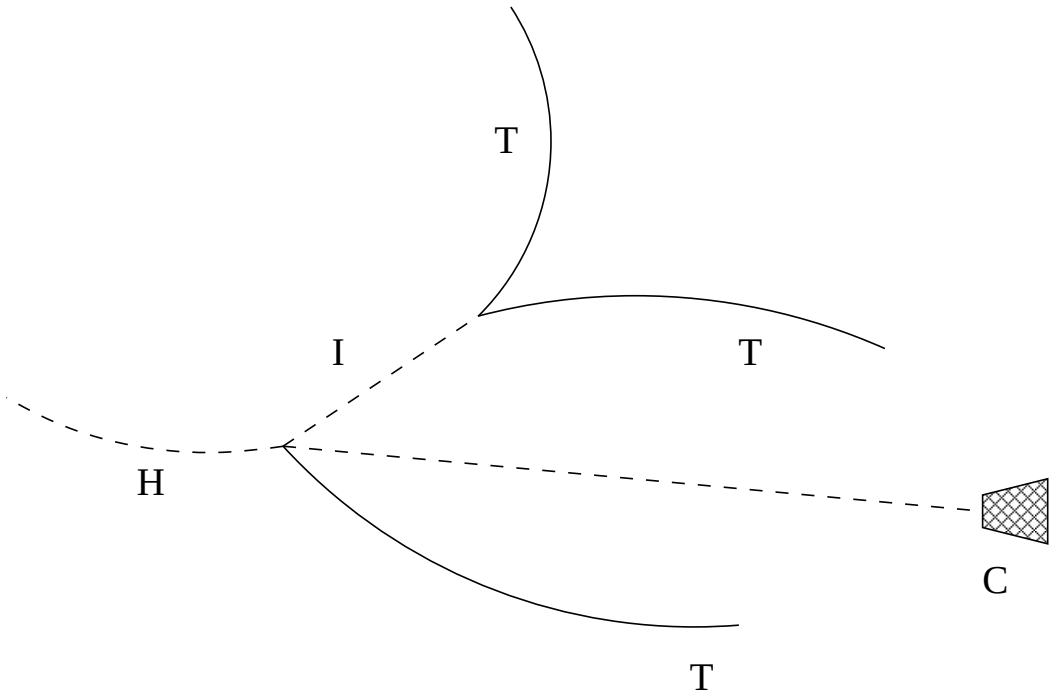

Fig. 1. Schematic picture of a decay tree with three charged particles reconstructed as track segments (T), one photon reconstructed as a calorimeter cluster (C), and two composite particles (I for 'internal' and H for 'head').

such as π^0, J/ψ and D^*, are treated as resonances. [1]

We distinguish two types of constraints in the decay tree. Two *internal* constraints are applied to remove redundant degrees of freedom: the vertex constraint expresses the relation between the decay vertex of a particle and the production vertex of its daughters; the momentum conservation constraint ensures four-momentum conservation at each vertex. The reconstructed final state particles constitute the *external* constraints. In this paper we consider only 5-parameter track segments and calorimeter clusters with a reconstructed position and energy. Explicit expressions for the constraints are given in section 4. To put those in the proper context we introduce the fit procedure first.

[1] We use the term resonance for any particle with a short lifetime, regardless of whether the decay is through the strong or electroweak interaction.

3 Fitting a decay tree

3.1 Measurement constraints and exact constraints

To extract the optimal set of decay tree parameters from the reconstruction information we use a least squares fit. Within this framework constraints are expressed as χ^2 contributions which are a function of the parameters of the model, collectively denoted by the vector x. The solution to the fit is the value of x that minimizes the total χ^2. To define the χ^2 contributions we distinguish between *exact* constraints and *measurement* constraints. The latter are characterized by the fact that they have an associated uncertainty, whereas the former do not. The internal constraints of the decay tree model are exact constraints, whereas the external constraints are measurement constraints.

For a measurement constraint i the χ^2 contribution takes the form

$$\chi^2_i \;=\; r_i^T(x)\;\; V_i^{-1}\; r_i(x) \tag{1}$$

where $r_i(x)$ is the constraint residual and V_i is the constraint variance. We use a matrix notation so that the χ^2 contribution is defined for constraints of any dimension. The residual can be defined as

$$r_i(x) \;=\; m_i \;-\; h_i(x) \tag{2}$$

where m_i is the value of the measured quantity (for example the parameters from a reconstructed track) and $h_i(x)$ is the measurement model that expresses this quantity in terms of the parameters x. With this definition V_i is the variance in the measurement m_i.

Exact constraints can be imposed on the model by parameter substitution. For example, the parameters that represent the momentum of a mother particle can directly be replaced by a sum over the daughter momenta. Although this simplifies the fitting problem by reducing the number of parameters, it is not suitable for the decay tree fit discussed here. First, the substitution procedure makes it more complicated to use recurrence in the implementation of the fitting algorithm. Second, it complicates the calculation of those parameters that have been removed — the momentum of the mother —, especially where it concerns the associated uncertainty.

Consequently, exact constraints are not applied by substitution but by means of Lagrange multipliers. If the exact constraint in terms of x is written as

$$g_i(x) \;=\; 0, \tag{3}$$

the χ^2 contribution of the constraint takes the form

$$\chi_i^2 \;=\; 2\,\lambda_i^T\,g_i(x) \tag{4}$$

where λ_i is the Lagrange multiplier. The latter is added to the list of parameters x for which we minimize the χ^2.

3.2 The standard least squares fit

The requirement that $\chi^2 = \sum_i \chi_i^2$ be minimal defines a set of equations $\partial\chi^2/\partial x = 0$. A solution can be obtained with a Newton-Raphson method. (See for example [1].) Given an initial estimate $x^{(0)}$, one obtains a new estimate

$$x^{(1)} \;=\; x^{(0)} - \left(\frac{\partial^2\chi^2}{\partial x^2}\right)^{-1}\frac{\partial\chi^2}{\partial x}. \tag{5}$$

For constraints that are not linear in x this expression can be applied iteratively until a certain convergence criterion is met. Using error propagation one can derive that the variance in x is given by

$$C(x) \;=\; 2\left(\frac{\partial^2\chi^2}{\partial x^2}\right)^{-1}. \tag{6}$$

We shall call the procedure described above, in which the χ^2 contributions of all constraints are minimized simultaneously, the *standard* fit. [2] The expressions for the standard fit show that the minimization procedure requires the inversion of matrices with the dimension of the parameter vector x. Complicated decay chains can easily require several tens of parameters, which leads to large computational costs.

3.3 The progressive least squares fit

The Kalman filter or *progressive* fit [2] is a χ^2 minimization method that is less computation intensive than the standard fit. In the reconstruction of data from particle physics experiments the Kalman filter is mainly applied in track fitting, where its virtue is not only speed, but also the possibility to easily

[2] This method for χ^2 minimization is often called a 'global' fit, but we reserve the term global in this paper for use in 'global decay chain fit', a decay chain fit that determine all parameters and correlations in a decay tree simultaneously, rather than leaf-by-leaf.

include multiple scattering effects as so called 'process noise' [3]. The Kalman filter has been proposed for vertex fitting by several other authors [3,4]. However, a general treatment of exact constraints has not been considered before, which justifies a re-derivation of the Kalman filter for the purpose of decay chain fitting. To connect with previous work we follow a notation close to that in [3].

Consider a measurement constraint k. Assume that the χ^2 consisting of all contributions of constraints $\{0, \ldots, k-1\}$ has already been minimized with respect to the model parameters, leading to a 'prediction' x_{k-1} with variance C_{k-1}. To calculate how x changes when the constraint k is included in the minimization, we define a χ^2 contribution

$$\begin{aligned}\chi^2_k \;=\; & (x - x_{k-1})^T \, {C_{k-1}}^{-1} \, (x - x_{k-1}) \\ & + (h_k(x) - m_k)^T \, {V_k}^{-1} \, (h_k(x) - m_k).\end{aligned} \tag{7}$$

The least squares solution for x is obtained from the requirement that $\partial\chi^2/\partial x \equiv 0$, *i.e.*

$$ {C_{k-1}}^{-1}(x - x_{k-1}) \;+\; H_k^T \, V_k^{-1} \, (h_k(x) - m_k) \;=\; 0 \tag{8}$$

where $H_k \equiv \partial h/\partial x|_{x_{k-1}}$ is the derivative or projection matrix. We call the solution to this equation the *updated* parameter vector x_k.

The authors of reference [3] discusses two approaches to calculate x_k, which are called the 'gain matrix formalism' and the 'weighted means formalism'. The latter still requires inversion of matrices with the dimension of x and is not suitable for our purposes. In the gain formalism one rewrites Eq. 8 as

$$\left({C_{k-1}}^{-1} + H_k^T {V_k}^{-1} H_k\right) (x - x_{k-1}) \;=\; H_k^T {V_k}^{-1} r_k^{k-1} \tag{9}$$

where we defined the so-called residual of the prediction

$$r_k^{k-1} = m_k - h_k(x_{k-1}) \tag{10}$$

and where we assumed that the measurement model is linear, *i.e.*

$$h_k(x) \;=\; h_k(x_{k-1}) \;+\; H_k \, (x - x_{k-1}). \tag{11}$$

The treatment of more general h will be discussed below. Solving for x, we obtain

$$x_k \;=\; x_{k-1} \;+\; K_k \, r_k^{k-1} \tag{12}$$

where the gain matrix K_k is defined as

$$K_k \;=\; \left({C_{k-1}}^{-1} + H_k^T {V_k}^{-1} H_k\right)^{-1} H_k^T {V_k}^{-1}. \tag{13}$$

The latter can be rewritten as

$$K_k \;=\; C_{k-1} H_k^T \left(R_k^{k-1}\right)^{-1} \tag{14}$$

where

$$R_k^{k-1} \;=\; V_k + H_k C_{k-1} H_k^T \tag{15}$$

is the uncertainty in the predicted residual. The fact that Eq. 14 contains the inverse of a matrix with the dimension of the measurement m_k, rather than with the dimension of the parameter vector x, is the reason that the progressive fit is in general faster than the standard fit.

The updated covariance matrix C_k can be obtained by error propagation from Eq. 12, which gives

$$C_k \;=\; (1 - K_k H_k)\, C_{k-1}\, (1 - K_k H_k)^T \;+\; K_k V_k {K_k}^T. \tag{16}$$

This expression is computation intensive because the first term on the right hand side corresponds to a product of three square matrices with the dimension of the parameter vector. It can be simplified to

$$C_k \;=\; (1 \;-\; K_k H_k)\, C_{k-1} \tag{17}$$

which is much faster, but known to be sensitive to finite machine digit accuracy, in particular if V_k is small compared to $H_k C_{k-1} H_k^T$ [5]. This can be understood by evaluating the effect of a small perturbation in the gain matrix $K_k \rightarrow K_k + \delta K$. Substituting this in Eq. 16 yields $\delta C_k = \delta K R_k \delta K^T$, whereas Eq. 17 gives $\delta C_k = -\delta K H_k C_k$. As a result the second expression can lead to a covariance matrix with a negative determinant, an effect that we indeed observed in fits with many parameters. We have found that by rewriting Eq. 16 as

$$C_k \;=\; C_{k-1} \;-\; K_k \left(2 H_k C_{k-1} \;-\; R_k^{k-1} K_k^T\right), \tag{18}$$

the computational stability is preserved at the cost of a moderate increase in computation time with respect to Eq. 17.

Finally, the χ^2 contribution of the constraint m_k is given by the χ^2 contribution of the prediction, *i.e.*

$$\chi_k^2 \;=\; (r_k^{k-1})^T (R_k^{k-1})^{-1} r_k^{k-1}. \tag{19}$$

The χ^2 contribution of a particular constraint depends on the order in which the constraints are applied. However, if all constraints are linear in x, the sum of the χ^2 contributions is independent of that order.

3.4 Non-linear constraints

If the measurement model is not linear in x, x_k can be extracted with an iterative procedure. Expanding $h(x)$ around a point $x^{(i)}$ (initially given by x_{k-1}),

$$h_k(x) \;=\; h_k(x^{(i)}) \;+\; H_k^{(i)}(x - x^{(i)}) \tag{20}$$

the estimate for x_k becomes

$$x_k^{(i+1)} \;=\; x_{k-1} \;+\; K_k^{(i)}\, r_k^{k-1(i)} \tag{21}$$

where the residual $r_k^{k-1(i)}$ is given by

$$r_k^{k-1(i)} \;=\; m_k - h_k(x^{(i)}) \;-\; H_k^{(i)}(x_{k-1} - x^{(i)}). \tag{22}$$

Choosing $x_k^{(i+1)}$ as the new expansion point, one obtains an improved estimate of x_k by iteration, subject to a certain convergence criterion. A suitable observable to test the convergence is the χ^2 contribution

$$\chi_k^{2\,(i)} \;=\; \left(r_k^{k-1(i)}\right)^T \left(R_k^{k-1(i)}\right)^{-1} r_k^{k-1(i)}. \tag{23}$$

The time consuming calculation of the covariance matrix (Eq. 16) can be performed after convergence is obtained.

3.5 Exact constraints

The χ^2 contribution for an exact constraint $g(x) = 0$ was introduced in Eq. 4. Minimization of the χ^2 under the exact constraint is performed by solving the set of equations $\partial\chi^2/\partial x = 0$ and $\partial\chi^2/\partial\lambda = 0$ for x and λ simultaneously. To derive the expressions for the progressive fit we define a χ^2

$$\chi_k^2 \;=\; (x - x_{k-1})^T {C_{k-1}}^{-1} (x - x_{k-1}) \;+\; 2\lambda_k^T\, g_k(x). \tag{24}$$

Linearizing the constraint equation around x_{k-1}

$$g_k(x) \;=\; g_k(x_{k-1}) \;+\; G_k\,(x - x_{k-1}) \;+\; \cdots \tag{25}$$

where $G = \partial g/\partial x$, we obtain for the linearized set of first derivatives

$$\begin{aligned} 0 \;&=\; {C_{k-1}}^{-1}(x - x_{k-1}) \;+\; G_k^T\lambda_k \\ 0 \;&=\; g_k(x_{k-1}) \;+\; G_k\,(x - x_{k-1}) \end{aligned} \tag{26}$$

Multiplying the first equation by GC_{k-1} and subtracting the second equation yields

$$(G_k C_{k-1} G_k^T)\, \lambda_k \;=\; g_k(x_{k-1}). \tag{27}$$

Since for non-trivial constraint equations the matrix on the left side is invertible, this equation leads to a solution for λ_k. Eliminating λ_k we obtain for the updated parameter vector

$$x_k \;=\; x_{k-1} \;-\; K_k\, g_k(x_{k-1}) \tag{28}$$

where we defined the gain matrix for exact constraints by

$$K_k \;=\; C_{k-1} G_k^T \left(G_k C_{k-1} G_k^T\right)^{-1}. \tag{29}$$

Using error propagation we obtain for the updated covariance matrix

$$C_k \;=\; (1 - K_k G_k)\, C_{k-1}\, (1 - K_k G_k)^T \tag{30}$$

and for the χ^2 contribution

$$\chi^2_k \;=\; g_k(x_{k-1})^T \left(G_k C_{k-1} G_k^T\right)^{-1} g_k(x_{k-1}). \tag{31}$$

A comparison of the equations for the exact constraint with those for the measurement constraint shows that with the substitutions

$$\begin{aligned} h(x_{k-1}) - m_k \;&\longrightarrow\; g_k(x_{k-1}) \\ V_k + H_k C_{k-1} H_k^T \;&\longrightarrow\; G_k C_{k-1} G_k^T \end{aligned} \tag{32}$$

the two procedures are identical. This non-trivial result confirms the intuitive notion that an exact constraint is effectively the same as a measurement with infinite precision.

The minus sign in equation Eq. 28 with respect to its counterpart Eq. 12 is the result of our decision to choose a conventional notation. It is customary to express the Kalman filter equations in terms of the derivate of $h(x)$ to x rather than the derivate of the residual $r(x)$ to x. The minus sign reflects the fact that these derivatives differ by a sign when the residual is defined as in Eq. 2. For the implementation of the fit we have defined the residual with opposite sign, such that the same expressions can be used for exact constraints and measurement constraints.

It is interesting that the progressive fit deals more effectively with exact constraints than the standard fit does. In the latter the Lagrange multipliers are added explicitly as parameters to the fit, increasing the number of parameters and therefore computational costs. The treatment of an exact constraint in

the standard fit is therefore relatively expensive. In the progressive fit the Lagrange multipliers can be eliminated and exact constraints are less expensive than measurement constraints.

4 Explicit expressions for constraints in the decay tree

In this section we provide explicit expressions for the internal and external constraints introduced in section 2.

4.1 The internal constraints

The internal constraints reduce the set of decay tree parameters to a set that is not overcomplete. In the absence of a magnetic field or for neutral particles, the momentum vector $\vec{p}$ is constant, leading to a time-evolution of the position $\vec{x}(t) = \vec{x}_0 + \vec{p}\,t/\gamma m$, where t is the time in the lab frame, m the rest mass and x_0 the position at $t = 0$. For each composite particle i in the decay tree the vertex constraint expresses the relation between its decay vertex $\vec{x}_i$, its momentum $\vec{p}_i$ and the decay vertex of its mother $\vec{x}_M$,

$$\vec{x}_M - \vec{x}_i + \theta_i \vec{p}_i \;=\; 0 \tag{33}$$

where $\theta \equiv l/|\vec{p}| = t/\gamma m$ is the decay time parameter. The momentum constraint for particle i can be expressed as

$$\vec{p}_i - \sum_j \vec{p}_j \;=\; 0 \qquad \text{and} \qquad E_i - \sum_j E_j \;=\; 0, \tag{34}$$

where the sum runs over the momenta of all the daughters.

For charged particles in a magnetic field the expressions for the internal constraints are more complicated. In most practical applications one can neglect the effect of the magnetic field for the particles inside the decay tree, because the bending in a typical lifetime is very small. This is for example the case for B and D mesons in the 1.5-T magnetic field of the *BABAR* detector. It is not true for some charged baryons such as $\Xi^{\pm}$ and $\Sigma^{\pm}$. The full expressions for the internal constraints in a constant magnetic field have been implemented for *BABAR* but are outside the scope of this paper.

The magnetic field in the *BABAR* spectrometer is approximately homogeneous and aligned with the z-axis of the detector. Reconstructed charged particle trajectories are represented by a 5 parameter helix $m^T \equiv (d_0, \phi_0, \omega, z_0, \tan\lambda)$ and a corresponding covariance matrix. In terms of these parameters, the position $\vec{x}$ and momentum $\vec{p}$ of the particle along the helix trajectory are given by

$$\begin{aligned} x &= r\sin(\phi) - (r + d_0)\sin(\phi_0) \\ y &= -r\cos(\phi) + (r + d_0)\cos(\phi_0) \\ z &= z_0 + l\tan(\lambda) \\ p_x &= p_t\cos(\phi) \\ p_y &= p_t\sin(\phi) \\ p_z &= p_t\tan(\lambda) \end{aligned} \tag{35}$$

where l is the flight length in the transverse plane, measured from the point of the helix closest to the z-axis, $\phi = \phi_0 + \omega l$, $r = 1/\omega$ and $p_t = qa/\omega$ with q the charge of the particle in units of the positron charge and $a[J/m] = -e[C]B_z[T]$ a constant. The measurement model $h(x)$ used in the decay tree fit follows from the inverse transformation and can be written as

$$h \equiv \begin{pmatrix} d_0 \\ \phi_0 \\ \omega \\ z_0 \\ \tan\lambda \end{pmatrix} = \begin{pmatrix} (p_{t0} - p_t)/aq \\ \mathrm{atan2}(p_{y0}, p_{x0}) \\ aq/p_t \\ z - lp_z/p_t \\ p_z/p_t \end{pmatrix} \tag{36}$$

with $p_t = \sqrt{p_x^2 + p_y^2}$, $p_{x0} = p_x + aqy$, $p_{y0} = p_y - aqx$, $p_{t0} = \sqrt{p_{x0}^2 + p_{y0}^2}$, $\phi = \mathrm{atan2}(p_y, p_x)$ and $l = (\phi - \phi_0)p_t/qa$. The derivatives can be concisely

written as

$$H^T \equiv \begin{pmatrix} \frac{\partial h^T}{\partial x} \\ \frac{\partial h^T}{\partial y} \\ \frac{\partial h^T}{\partial z} \\ \frac{\partial h^T}{\partial p_x} \\ \frac{\partial h^T}{\partial p_y} \\ \frac{\partial h^T}{\partial p_z} \end{pmatrix} = \begin{pmatrix} \frac{-p_{y0}}{p_{t0}} & \frac{-aqp_{x0}}{p_{t0}^2} & 0 & \frac{-p_z p_{x0}}{p_{t0}^2} & 0 \\ \frac{p_{x0}}{p_{t0}} & \frac{-aqp_{y0}}{p_{t0}^2} & 0 & \frac{-p_z p_{y0}}{p_{t0}^2} & 0 \\ 0 & 0 & 0 & 1 & 0 \\ \frac{1}{aq}\left(\frac{p_{x0}}{p_{t0}} - \frac{p_x}{p_t}\right) & \frac{-p_{y0}}{p_{t0}^2} & \frac{-aqp_x}{p_t^3} & \frac{-p_z}{aq}\left(\frac{p_{y0}}{p_{t0}^2} - \frac{p_y}{p_t^2}\right) & \frac{-p_z p_x}{p_t^3} \\ \frac{1}{aq}\left(\frac{p_{y0}}{p_{t0}} - \frac{p_y}{p_t}\right) & \frac{p_{x0}}{p_{t0}^2} & \frac{-aqp_y}{p_t^3} & \frac{p_z}{aq}\left(\frac{p_{x0}}{p_{t0}^2} - \frac{p_x}{p_t^2}\right) & \frac{-p_z p_y}{p_t^3} \\ 0 & 0 & 0 & -\frac{l}{p_t} & \frac{1}{p_t} \end{pmatrix}. \quad (37)$$

4.3 The reconstructed cluster constraint

In *BABAR* reconstructed calorimeter clusters are represented by a measured position and energy $m^T = (\vec{x}_{\rm clus}, E_{\rm clus})$ and a corresponding covariance matrix $V_{\rm clus}$. Given a mother decay vertex $\vec{x}$ and a momentum vector $\vec{p}$, the measurement model is defined as

$$h = \begin{pmatrix} x + \theta p_x \\ y + \theta p_y \\ z + \theta p_z \\ \sqrt{p_x^2 + p_y^2 + p_z^2} \end{pmatrix} \quad (38)$$

where θ takes the role of the photon 'decay length'. In principle, θ can be added to the photon parameter list and extracted from the fit. Since this parameter is not very interesting, it is preferable to eliminate it. This can be done by reducing the set of four constraint equations $r(x) \equiv m - h(x) = 0$ to three by redefining the residual, for example

$$r'(x) \equiv \begin{pmatrix} (x_{\rm clus} - x)p_y - (y_{\rm clus} - y)p_x \\ (x_{\rm clus} - x)p_z - (z_{\rm clus} - z)p_x \\ E_{\rm clus} - \sqrt{p_x^2 + p_y^2 + p_z^2} \end{pmatrix}. \quad (39)$$

The choice of r' is not unique: This particular choice is not suitable if p_x is zero, because the two position constraints would no longer be independent. However, for every value of $\vec{p}$ a set of independent constraints can be constructed. The variance of the new constraint is simply given by

$$V' = P\, V_{\rm clus}\, P^T \quad (40)$$

where $P = \partial r'/\partial m$ is the derivate of the constraint to the measurement.

4.4 Other constraints

The constraints discussed above constitute the minimal set of constraints necessary for fitting a decay tree with final state particles that are reconstructed either as charged tracks or as calorimeter clusters. We have considered and implemented several other constraints. Sometimes, position and momentum parameters can be improved by constraining the mass of composites in the decay tree to the known particle mass. Knowledge about the interaction point can be used to constrain the production vertex of the head of the decay tree. Information about the beam momenta can be used to constrain the four-vector of the head of the decay tree, *e.g.* in $e^+e^- \to \Upsilon(4S) \to B^0\overline{B}^0$ decays. In addition to charged tracks and photons, we have used reconstructed K^0_L particles which are detected in the *BABAR* calorimeter, but for which the deposited energy is not useful as an estimate of the magnitude of the momentum. Finally, we have found that missing particles can be included in the decay tree, provided the tree is not kinematically under-constrained. The expressions for these constraints are easy to derive so we will not include them in this paper.

4.5 Ordering constraints

A disadvantage of the progressive fit with respect to the standard fit is that the final result of the fit can be sensitive to the order in which constraints are applied. In fits with 'process noise' such as track fits, there is a natural ordering. However, in fits without process noise, the ordering of the constraints can be chosen freely.

The order in which constraints that are linear in x are applied is irrelevant, because the covariance matrix contains all essential information on the constraint derivatives. If, for example, a constraint k is processed such that $g_k(x_k) = 0$, then $g_k(x_n) = 0$ for any $n > k$. This is not the case for non-linear constraints, since the covariance matrix does not contain information on the higher derivatives of the constraint equation. Consequently, the order in which constraints are applied becomes important: The most non-linear constraints should be applied last.

One can consider applying correlated non-linear constraints simultaneously, rather than consecutively. For example, the vertex constraint can be applied separately in the three space coordinates x, y and z. However, the dependence on the decay time parameter θ correlates these constraints. Since they are also slightly non-linear, it is preferable to treat them as a single three-dimensional constraint rather than three separate one-dimensional constraints. Ultimately, all constraints can be applied simultaneously, which effectively reduces the

progressive fit to a standard fit. The performance advantage of the progressive fit then practically disappears. [3]

Based on these considerations we have chosen the following approach to ordering and combining constraint. The external constraints (reconstructed tracks and cluster, constraints to the interaction point etc.) are treated first. Subsequently, all four-momentum conservation constraints are applied, starting at the end of the decay tree. Finally, at each vertex the geometric constraints and an eventual mass are combined. These combined constraints are applied consecutively starting at the end of the decay tree.

4.6 Fit initialization and convergence

The progressive fit requires initialization of both the parameters x_0 and the covariance matrix C_0. Vertex positions are initialized with the average interaction point or with the point of closest approach of (a subset of) reconstructed track segments in the decay tree. The momenta of particles reconstructed as a track segments are initialized by evaluating the track parameters at the point of closest approach to the initial vertex positions. The momenta of photons are initialized by using the initial vertex positions as their origin. Particle momenta inside the decay tree are initialized by adding the initial four vectors of their daughters. Finally, the decay time parameters are initialized from the initial vertex positions and momenta or from the expected decay time.

The covariance matrix must be initialized with uncertainties that are large enough that the initial parameters have a negligible weight in the final result of the fit, yet small enough that the measurement errors V_k in equation are not numerically negligible with respect to $H_k C_k H_k^T$. We have chosen for a diagonal matrix with diagonal elements that are roughly a factor 1000 larger than the square of the typical resolution for the corresponding parameter.

Even with the iteration of non-linear constraints described in section 3.4 the decay chain fit does not converge in a single processing of all constraints. Therefore, we repeat the fit procedure until the total χ^2 is stable. At each step x_0 is initialized with the result of the previous step, while C_0 is reset to its original value. Fits typically converge in three iterations.

[3] The progressive fit still has the advantage that exact constraints do not lead to extra (Lagrange multiplier) parameters.

5 Experience in *BABAR*

We have implemented the decay chain fit described in the previous sections in the *BABAR* analysis framework. The fit has been extensively tested and is used in a variety of physics analyses. It is a useful alternative for leaf-by-leaf vertex fits, in particular for the reconstruction of decay chains with vertices with insufficient downstream constraints, such as $\Xi^0 \to \Lambda^0\pi^0$ and $K^0_S \to \pi^0\pi^0$, consistent treatment of mass constraints at several levels in a decay tree, direct extraction of the $B^0\overline{B}^0$ decay time difference for analysis of time-dependent *CP* violation in $\Upsilon(4S) \to B^0\overline{B}^0$ events and kinematic fits with missing particles. We briefly discuss two examples.

Figure 2a shows the $c\tau$ distribution of D^+ candidates in a *BABAR* simulation of $\overline{B}^0 \to D^+\pi^-$ decays with $D^+ \to K^-\pi^+\pi^+$. Only candidates that are matched to the Monte Carlo truth are shown. The average reconstructed lifetime is close to the average lifetime $c\tau_{D^+} = 0.311\,\mathrm{mm}$ with which the events were generated. Figure 2b shows the $c\tau$ pull distribution, which has an RMS consistent with one.

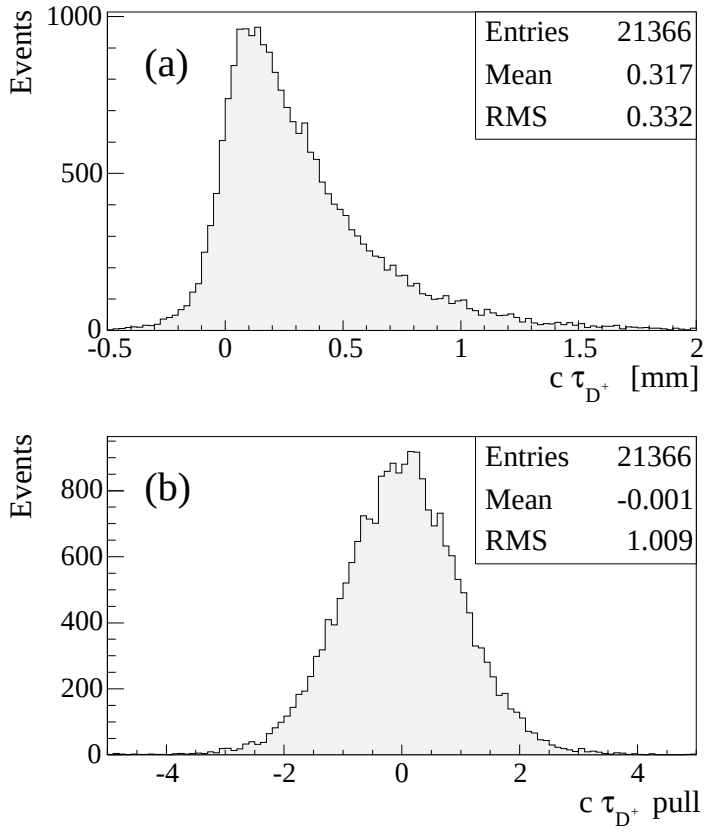

Fig. 2. Reconstructed lifetime (a) and lifetime pull (b) for $D^\pm$ extracted from a global decay chain fit to simulated $\overline{B}^0 \to D^+\pi^-$ ($D^+ \to K^-\pi^+\pi^+$) decays.

As a second example, we study the reconstruction of $K^0_S \to \pi^0\pi^0$ candidates in simulated $B^0 \to J/\psi K^0_S$ decays with $\pi^0 \to \gamma\gamma$ and $J/\psi \to \mu^+\mu^-$. The $K^0_S \to \pi^0\pi^0$ decay cannot be reconstructed with *BABAR*'s traditional leaf-by-leaf fit. A global decay tree fit can be performed, provided that the origin of the K^0_S is known and that mass constraints are applied to the π^0 candidates. In this particular topology the J/ψ vertex provides the origin and the $B^0 \to J/\psi K^0_S$ fit is thus sufficiently constrained.

Figure 3a shows the invariant mass distribution of the $K^0_S \to \pi^0\pi^0$ candidates extracted from a fit to the $B^0 \to J/\psi K^0_S$ decay tree. The central value and resolution are significantly better than for the 'raw' $\pi^0\pi^0$ invariant mass distribution that was obtained by assuming that the π^0 decays originate directly from the $J/\psi \to \mu^+\mu^-$ vertex. Figure 3b shows the χ^2 consistency of the $B^0 \to J/\psi K^0_S$ decay tree fit. (The χ^2 has two degrees of freedom.) It is not entirely consistent with a flat distribution, partially because the energy of the photons originating from the π^0 candidates is not always fully reconstructed in the *BABAR* calorimeter.

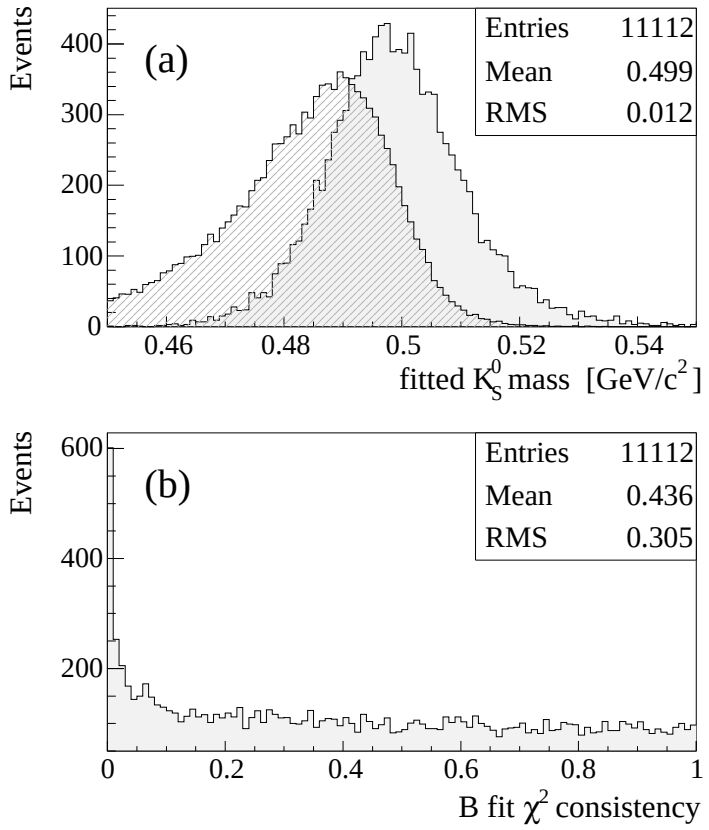

Fig. 3. $K^0_S \to \pi^0\pi^0$ invariant mass (a) extracted from a global decay chain fit to simulated $B^0 \to J/\psi K^0_S$ decays and the χ^2 consistency of the fit (b). The hashed distribution in figure (a) is the $\pi^0\pi^0$ invariant mass before the geometric fit is performed.

The performance of the fit has been compared to a traditional leaf-by-leaf vertex fit that has been used in *BABAR* for several years. A direct comparison of computational performance is not trivial since that depends on implementation choices in addition to the algorithmic complexity of the problem. The complexity of the global decay chain fit grows roughly with the square of the number of vertices in the decay chain, whereas the leaf-by-leaf fits (which do not keep track of correlations) behave more linear. Despite this fact, computation time use has not been a limitation in practical applications of the fit.

6 Acknowledgment

The author would like to thank Dr. D.N. Brown, Dr. W.T. Ford and Dr. A. Jawahery for their help in preparing this document. The work described here was supported by the U.S. Department of Energy under grant number DEFG02-96ER41015.

References

[1] R. Bock and W. Kirscher, *The Data Analysis BriefBook* (Springer-Verlag, Berlin, Heidelberg, New York, 1998).

[2] R. Kalman, Journal of Basic Engineering , 35 (1960).

[3] R. Frühwirth, Nucl. Instrum. Methods Phys. Res. **A262**, 444 (1987).

[4] R. Luchsinger and C. Grab, Comput. Phys. Commun. **76**, 263 (1993).

[5] See for example page 305 in A. Gelb, *Applied Optimal Estimation* (MIT Press, 1974).